Ann. Geophys., 33, 1413–1419, 2015
www.ann-geophys.net/33/1413/2015/
doi:10.5194/angeo-33-1413-2015

Annales Geophysicae Open Access EGU

Non-elliptic wavevector anisotropy for magnetohydrodynamic turbulence

Y. Narita[1,2]

[1]Space Research Institute, Austrian Academy of Sciences, Schmiedlstr. 6, 8042 Graz, Austria
[2]Institut für Geophysik und extraterrestrische Physik, Technische Universität Braunschweig, Mendelssohnstr. 3, 38106 Braunschweig, Germany

Correspondence to: Y. Narita (yasuhito.narita@oeaw.ac.at)

Received: 29 June 2015 – Revised: 24 October 2015 – Accepted: 3 November 2015 – Published: 13 November 2015

Abstract. A model of non-elliptic wavevector anisotropy is developed for the inertial-range spectrum of magnetohydrodynamic turbulence and is presented in the two-dimensional wavevector domain spanning the directions parallel and perpendicular to the mean magnetic field.

The non-elliptic model is a variation of the elliptic model with different scalings along the parallel and the perpendicular components of the wavevectors to the mean magnetic field.

The non-elliptic anisotropy model reproduces the smooth transition of the power-law spectra from an index of -2 in the parallel projection with respect to the mean magnetic field to an index of $-5/3$ in the perpendicular projection observed in solar wind turbulence, and is as competitive as the critical balance model to explain the measured frequency spectra in the solar wind. The parameters in the non-elliptic spectrum model are compared with the solar wind observations.

Keywords. Interplanetary physics (MHD waves and turbulence; solar wind plasma) – space plasma physics (turbulence)

1 Introduction

The spatial structure of space and astrophysical plasma turbulence is fundamentally different from that of ordinary fluid turbulence because the large-scale magnetic field imposes a special direction, causing anisotropy in the energy spectrum in the wavevector domain. On spatial scales larger than the ion gyro-radius and inertial length, the behavior of plasmas can be treated as magnetohydrodynamics (MHD). Evidence for anisotropy in MHD turbulence can be found in numerical simulations (Shebalin et al., 1983), correlation functions of interplanetary magnetic field fluctuations (Matthaeus et al., 1990; Dasso et al., 2005), and mean free paths in galactic cosmic ray diffusion (Bieber et al., 1994, 1996). Naively speaking, anisotropy is explained by three-wave interactions of obliquely propagating Alfvén waves such that the parallel component of the wavevector remains either zero or constant through the energy cascade (Biskamp, 2003).

Various models have been proposed to explain or reproduce the anisotropic energy spectra in the wavevector domain: the density fluctuation model (Higdon, 1984), the critical balance model by regulating the Alfvén wave interaction time with the eddy turnover time (Goldreich and Sridhar, 1995, 1997; Forman et al., 2011), generalization of critical balance by adding damping (von Papen and Saur, 2015); two-component model consisting of slab geometry and quasi-two-dimensional turbulence (Matthaeus et al., 1990; Bieber et al., 1996), the three-component model as an extension of the two-component model by adding the compressible fluctuation component (Matthaeus and Ghosh, 1999), the cross-helicity model showing asymmetry in the energy spectrum between the parallel and the anti-parallel directions to the mean magnetic field (Chandran, 2008), and the elliptic anisotropy model parameterized by the shape coefficients (Carbone et al., 1995).

Single-spacecraft measurements show that the magnetic energy spectra in the frequency domain (in the spacecraft frame) have different values of the spectral index in the range from -2 to $-5/3$ when the flow is quasi-parallel and quasi-perpendicular to the mean magnetic field, respectively (Horbury et al., 2008; Osman and Horbury, 2009). Although the spectra are measured in the frequency domain, the angle de-

AnGeo Communicates

pendence of the spectral index is valid in the streamwise wave-number domain regardless of the validity of Taylor's frozen-in-flow hypothesis within the random sweeping treatment (Wilczek and Narita, 2012).

The critical balance model is so far known to explain the dependence of the spectral index on the angles between the flow direction and the mean magnetic field direction in solar wind turbulence. Forman et al. (2011) successfully fit the critical balance model to the results of Horbury et al. (2008), and the only free parameter that controlled the anisotropy is the outer spatial scale of turbulence L. The kinetic extension of the critical balance model can also reproduce the angle dependence (von Papen and Saur, 2015). The other spectral models cannot explain the angle dependence. For example, the two-component or three-component models assume that the wavevectors are confined to either quasi-parallel or quasi-perpendicular directions to the mean magnetic field. The one-dimensional spectral curves do not provide the power law. The elliptic spectrum provides a reasonable fit to the energy spectrum in the three-dimensional wavevector domain, but the measured wave-number range is limited to about 1 order of magnitude due to the limitation by the four-point sampling in space. Furthermore, as shown below, the elliptic spectral model implies that the power-law index of the one-dimensional spectra is invariant to the angle of integration. Is there any other spectral model that explains the measured angle dependence of the solar wind turbulence spectrum? This question is the motivation of this paper.

Here we develop a non-elliptic model of wavevector anisotropy for the inertial-range spectrum of MHD turbulence. The non-elliptic anisotropy is obtained as a generalization of the elliptic anisotropy by including different scalings along the parallel and the perpendicular components of the wavevectors to the mean magnetic field. It is worth noting that the multi-spacecraft measurements in the solar wind do not provide strong evidence for the critical balance so far, but the wavevector spectrum is of elliptic type or nearly elliptic (Narita, 2014). The critical balance model can successfully explain the angle dependence of the spectral index (Forman et al., 2011) at the cost of several (explicit or implicit) assumptions: (1) co-existence of the eddies and the Alfvén waves, (2) self-regulation of the energy cascade, and (3) axial symmetry. The first item (the co-existence) means that both the eddies in the perpendicular plane and the parallel (or obliquely) propagating Alfvén waves are present in MHD turbulence. Dispersion relation studies using multi-spacecraft data in the solar wind from the MHD to the ion kinetic ranges show that the wave frequencies in the plasma rest frame cannot be associated with either the eddies (identified as the zero-frequency mode) or the obliquely propagating Alfvén waves but rather with the sideband waves (Narita et al., 2011a; Perschke et al., 2013, 2014). The second item (the self-regulation) means that the major or predominant wavevector directions become increasingly oblique to the mean magnetic field on smaller spatial scales (or at higher wave numbers). The wavevector analysis using the Cluster data shows that the wavevectors are already quasi-perpendicular on both the MHD and the ion kinetic ranges (Narita et al., 2011a). The third item (the axial symmetry) means that the fluctuating magnetic field is axially symmetric (or gyrotropic) in the directions around the mean magnetic field due to the presence of eddies. Both single-spacecraft and multi-spacecraft observations in the solar wind show that the axial symmetry is violated in the distribution of the wavevectors and in the sense of fluctuating fields (Narita et al., 2010, 2011b; Chen et al., 2012). Therefore, we look for a model of anisotropic energy spectrum without incorporating the critical balance. The non-elliptic model is competitive for explaining the angle dependence of the spectral index in solar wind turbulence as the critical balance model does.

The non-elliptic spectrum model is important because it expands the list of possible models to explain the spectral anisotropy in the solar wind.

The currently known spectral models cannot account for the observation of a nearly elliptic formation of the energy spectra in the wavevector domain in solar wind turbulence showing a transition of the spectral extension from the parallel direction to the mean magnetic field into the perpendicular direction (Narita, 2014).

In particular, although the critical balance model was successfully applied to explaining solar wind turbulence essentially using one free parameter (except for the degree of freedom in the positive symmetric function), the model relies on both assumptions that obliquely propagating Alfvén waves co-exist with eddies and that an axially symmetry exists in the directions around the mean magnetic field. The direct measurements of the dispersion relations using the Cluster spacecraft data indicate that obliquely propagating Alfvén waves unlikely exist (or at least do not occur on the analyzed time intervals) both in the MHD and the kinetic ranges (Narita et al., 2011a; Perschke et al., 2013, 2014). The direct measurements of the energy spectra in the wavevector domain in the solar wind show nearly elliptic formation of the spectra with the broken axial symmetry around the mean magnetic field (Narita et al., 2011b, 2014).

The advantage of the non-elliptic model is in its mathematical construction. The spectral anisotropy in the wavevector domain is described. The model does not require assumption of any particular wave modes or fluctuation types such as Alfvén waves or eddies.

The non-elliptic model is particularly suited for testing in the solar wind, since the angle dependence of the spectral slopes has been studied in detail using in situ spacecraft measurements. The model is constructed as an inertial-range spectrum for MHD turbulence. Applications to laboratory plasmas and astrophysical plasmas are in principle possible, too.

2 Model construction

2.1 Elliptic anisotropy

Elliptic shape of the energy spectrum in the two-dimensional wavevector domain is constructed as a natural extension of the isotropic spectrum by introducing the shape coefficients, $c_\perp$ and $c_\parallel$, as

$$E(k_\perp, k_\parallel) = E_0\left(c_\perp k_\perp^2 + c_\parallel k_\parallel^2\right)^{-\alpha/2}, \quad (1)$$

where $k_\perp$ and $k_\parallel$ are the perpendicular and parallel components of the wavevector, respectively, and α the spectral index (see, e.g., Eq. 22 in Carbone et al., 1995).

Note that polarizations in the elliptic model by Carbone et al. (1995) are not considered here, as the goal of the paper is to construct a non-elliptic model for the total fluctuation energy (i.e., the trace of the cross-spectral density matrix). Construction of an elliptic model for the cross spectral density matrix may be possible, but it is beyond the scope of the current work.

To simplify the argument, the other coefficients in the inertial-range spectrum such as the Kolmogorov or Iroshikov–Kraichnan constant (Kolmogorov, 1941; Iroshnikov, 1964; Kraichnan, 1965) and the energy transfer rate ϵ are renormalized to E_0 in Eq. (1).

The elliptic spectrum assumes a symmetry with respect to changing the sign of the wavevector components, i.e., the cross helicity is implicitly zero. The scale invariance holds under the transformation $k_\perp \to \lambda k_\perp$ and $k_\parallel \to \lambda k_\parallel$. One-dimensional spectra are obtained by integrating the elliptic spectrum over the wavevector components:

$$E(k_\perp) = E_0 \int_{-\infty}^{\infty} \mathrm{d}k_\parallel\, E(k_\perp, k_\parallel) = E_0 C_1 k_\perp^{-\alpha+1}, \quad (2)$$

$$E(k_\parallel) = E_0 \int_{-\infty}^{\infty} \mathrm{d}k_\perp\, E(k_\perp, k_\parallel) = E_0 C_2 k_\parallel^{-\alpha+1}, \quad (3)$$

where C_1 and C_2 (and also C_3 and C_4 in the next subsection) denote the spectral amplification factors that determine the spectral energy in the one-dimensional wave-number domain in different directions with respect to the mean magnetic field.

The coefficient C_1 is evaluated using Euler's gamma function as

$$\begin{aligned} C_1 &= 2c_\perp^{-\alpha/2} \int_0^{\infty} \mathrm{d}\xi \left(1 + \frac{c_\parallel}{c_\perp}\xi^2\right)^{-\alpha/2} \\ &= a^{-\alpha/2} \sqrt{\frac{c_\perp \pi}{c_\parallel}} \frac{\Gamma(-\frac{1}{2} + \frac{\alpha}{2})}{\Gamma(\frac{\alpha}{2})}. \end{aligned} \quad (4)$$

The coefficient C_2 is obtained by exchanging $c_\perp$ by $c_\parallel$ in C_1. Here we assumed an inertial-range spectrum spanning to infinity in the wavevector domain. The one-dimensional spectra are expressed as a power law and, furthermore, the spectral index is the same between the two spectra. The isotropic spectrum is restored by taking the limit $c_\perp/c_\parallel \to 1$, and Kolmogorov's inertial-range spectrum is restored by comparing the spectral index of the one-dimensional spectrum as $-\alpha+1 = -5/3$. An important property of the elliptic anisotropy is that the existence of anisotropy cannot be measured solely from the analysis of the spectral indices because the effect of anisotropy appears in the coefficients, not in the spectral slope. To verify the elliptic anisotropy using one-dimensional spectra, one needs to measure the spectra both in the perpendicular and parallel directions to the large-scale magnetic field simultaneously.

2.2 Non-elliptic anisotropy

The power-law index of the frequency spectra in the solar wind has been found to depend on the angle of the flow (streamwise direction) from the large-scale magnetic field (Horbury et al., 2008; Osman and Horbury, 2009): $-5/3$ for the quasi-perpendicular angles and -2 for the quasi-parallel angles. Although the energy spectra of solar wind turbulence are measured in the frequency domain, the Eulerian frequency spectrum retains the same power law as that of the streamwise wave-number spectrum even under a large-scale flow variation which causes the Doppler broadening (Wilczek and Narita, 2012). Therefore, the dependence of the spectral index as a function of the angles from the large-scale magnetic field should be regarded as valid both in the frequency and streamwise wave-number domains.

We construct a non-elliptic wavevector spectrum by generalizing the quadratic dependence of one of the wavevector components. We seek a generalization of the dependence on the parallel wavevector component and replace $k_\parallel^2$ by $|k_\parallel|^\mu$ in Eq. (1) because the spectral decay is steeper in the parallel wave numbers. One-dimensional spectra turn out to again be power laws, but the spectral indices now depend on the parameter μ as

$$E(k_\perp) = E_0 C_3 k_\perp^{-\alpha+\frac{2}{\mu}}, \quad (5)$$

$$E(k_\parallel) = E_0 C_4 k_\parallel^{-\frac{\mu}{2}(\alpha-1)}. \quad (6)$$

Here again, the coefficients C_3 and C_4 denote the spectral amplification factors that determine the spectral energies in the one-dimensional wave-number domain.

The coefficients C_3 and C_4 are again evaluated using the gamma function as

$$\begin{aligned} C_3 &= \frac{4c_\perp^{-\alpha}}{\mu} \int_0^{\infty} \mathrm{d}\xi \left(1 + \frac{c_\parallel}{c_\perp}\xi^2\right)^{-\alpha/2} \xi^{-1+\frac{2}{\mu}} \\ &= 2c_\perp^{-\alpha} \left(\frac{c_\perp}{c_\parallel}\right)^{1/\mu} \frac{\Gamma\left(\frac{\alpha}{2} - \frac{1}{\mu}\right)\Gamma\left(1 + \frac{1}{\mu}\right)}{\Gamma\left(\frac{\alpha}{2}\right)}, \end{aligned} \quad (7)$$

$$C_4 = 2c_\parallel^{-\alpha/2}\int_0^\infty \mathrm{d}\xi \left(1+\frac{c_\perp}{c_\parallel}\xi^2\right)^{-\alpha/2}$$
$$= c_\parallel^{-\alpha/2}\sqrt{\frac{c_\parallel \pi}{c_\perp}}\frac{\Gamma\left(-\frac{1}{2}+\frac{\alpha}{2}\right)}{\Gamma\left(\frac{\alpha}{2}\right)}. \quad (8)$$

Matching the power-law indices with the measured power laws, $k_\perp^{-5/3}$ and $k_\parallel^{-2}$, yields $\mu = 3$ and $\alpha = 7/3$. The non-elliptic wavevector spectrum for MHD turbulence $E(k_\perp, k_\parallel)$ in the solar wind is thus

$$E(k_\perp, k_\parallel) = E_0\left(c_\perp k_\perp^2 + c_\parallel |k_\parallel|^3\right)^{-7/6}. \quad (9)$$

3 Properties and application

3.1 Parameter study

Figure 1 displays four distinct cases of the non-elliptic spectra: case (a), with $c_\perp = 10^{-4}c_\parallel$; case (b), with $c_\perp = 10^{-5}c_\parallel$; case (c), with $c_\perp = 10^{-6}c_\parallel$; and case (d), with $c_\perp = 10^{-7}c_\parallel$.

The values are motivated by the direct measurements of the wavevector spectra (Narita, 2014).

The wave-number range is representative of the MHD range in the solar wind, well below the ion inertial wave number for protons at about 10^{-2} rad km^{-1}.

The Alfvén speed is typically in the range between 30 and 50 km s^{-1}, and the ion gyro-frequency is in the range from 0.5 to 1 rad s^{-1} in the solar wind near 1 AU (e.g., Perschke et al., 2014). Therefore, the variation in the ion inertial wave number is in the range from about 0.01 to 0.03 rad km^{-1}. The ion gyro-radius is in the same range for ion beta of unity (also typical in the solar wind at 1 AU; see Perschke et al., 2014).

Anisotropy is moderate in case (a) and becomes clearer at smaller ratios of the coefficients $c_\perp/c_\parallel$ with the spectral extension in the perpendicular directions to the mean magnetic field. Inspection of the spectra in Fig. 1 shows a transition of the spectral anisotropy. The spectra are extended in the parallel direction at lower wave numbers and perpendicular at higher wave numbers. The anisotropy transition is clearest in case (a).

3.2 One-dimensional spectra

Two-dimensional spectra are rotated around the axis at $(k_\perp, k_\parallel) = (0, 0)$ to transform the coordinate system into the k_x–k_z plane (i.e., rotation within the $k_\perp$–$k_\parallel$ plane) with a projection angle θ_{VB} between the flow direction and the mean magnetic field direction.

The transformation of the wavevector components (or the coordinate system) is given by the following relations:

$$k_\perp = \cos(\theta_{\mathrm{VB}})\, k_z - \sin(\theta_{\mathrm{VB}})\, k_x, \quad (10)$$
$$k_\parallel = \sin(\theta_{\mathrm{VB}})\, k_z + \cos(\theta_{\mathrm{VB}})\, k_x. \quad (11)$$

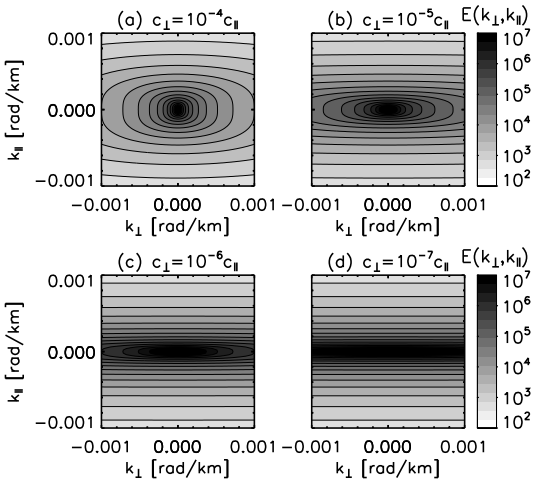

Figure 1. Two-dimensional energy spectrum for non-elliptic anisotropy (Eq. 9) for four coefficient sets: **(a)** $c_\perp = 10^{-4}c_\parallel$, **(b)** $c_\perp = 10^{-5}c_\parallel$, and **(c)** $c_\perp = 10^{-6}c_\parallel$, and **(d)** $c_\perp = 10^{-7}c_\parallel$. Wave-number range is chosen as representative of magnetohydrodynamic turbulence in the solar wind. The color bar is the spectral energy in the 2-D wavevector domain in units of nT^2 (rad km^{-1})$^{-2}$.

Note that we measure the angle θ_{VB} from the mean magnetic field direction. The spectra in the k_x–k_z plane are obtained with

$$E(k_x, k_z) = \Big[c_\perp |\cos(\theta_{\mathrm{VB}})\, k_z - \sin(\theta_{\mathrm{VB}})\, k_x|^2 + c_\parallel |\sin(\theta_{\mathrm{VB}})\, k_z + \cos(\theta_{\mathrm{VB}})\, k_x|^3\Big]^{-7/6} \quad (12)$$

and then integrated numerically over k_z to obtain the one-dimensional spectra at the projection angle θ_{VB} as

$$E(k_x) = \int_{-k_0}^{+k_0} \mathrm{d}k_z\, E(k_x, k_z), \quad (13)$$

where k_x represents the streamwise component of the wavevectors and k_z the perpendicular component to the flow.

The model is constructed as an inertial-range spectrum for MHD turbulence. It is assumed that the inertial range is infinitely long in the integration over the wavevector components.

The limit of the integration range is set to $k_0 = 100k_x$, above which the integration shows an asymptotic behavior. The integral is evaluated using Simpson's formula (Abramowitz and Stegun, 1972). Figure 2 displays the one-dimensional spectra in the streamwise wave-number domain $E(k_x)$ for projection angles $\theta_{\mathrm{VB}} = 0°, 10°, \cdots, 90°$. We obtain the results that the one-dimensional spectra show a power law in the streamwise wave-number domain, and that the power-law index varies smoothly from -2 at $\theta_{\mathrm{VB}} = 0°$ (in gray) to $-5/3$ at $\theta_{\mathrm{VB}} = 90°$ (in black) in all four cases.

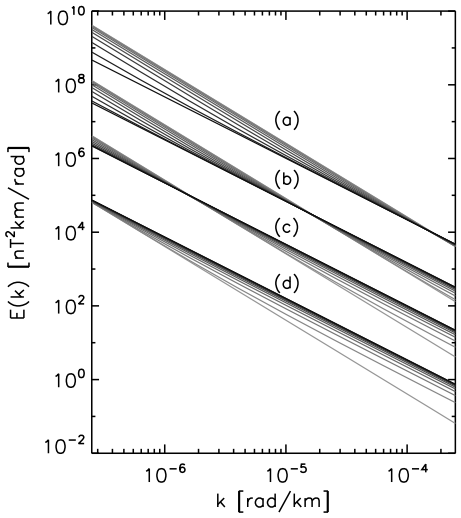

Figure 2. One-dimensional streamwise energy spectra obtained from the non-elliptic two-dimensional spectra for the four coefficient sets shown in Fig. 1. The spectra are obtained for projection angles θ_{VB} from the mean magnetic field from 0° (parallel projection, in gray) to 90° (perpendicular projection, in black) at 10° steps. The spectra are shifted on the logarithmic scale to separate among the four cases.

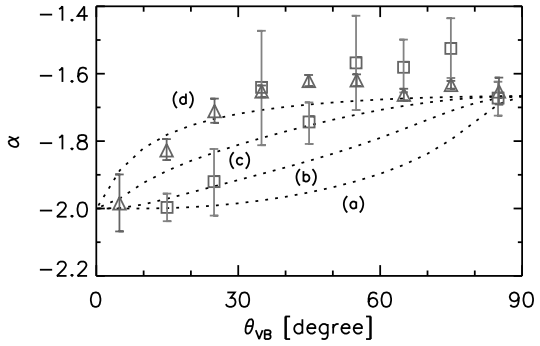

Figure 3. Power-law index α of the one-dimensional streamwise energy spectra as a function of the projection angles from the mean magnetic field θ_{VB} obtained from the non-elliptic anisotropy for four coefficient sets shown in Fig. 1, and that from single-spacecraft measurements of the frequency spectra in the solar wind presented by Horbury et al. (2008) (triangles in gray) and Osman and Horbury (2009) (squares in gray).

3.3 Test against solar wind data

Variation in the spectral index is studied quantitatively as a function of the projection angle θ_{VB} in Fig. 3.

The wave-number range from 2.5×10^{-7} to 2.5×10^{-4} rad km^{-1} (see Fig. 2) is used in the analysis of the spectral slopes, in which the slope determination is sufficiently accurate in the calculation.

The transition from a slope of -2 to $-5/3$ occurs at smaller angles from the mean magnetic field when the anisotropy is stronger. The transition angle is measured by the crossing of an index of 1.8: case (a) ($c_\perp = 10^{-4}c_\parallel$) shows the transition at 70 to 80°, case (b) ($c_\perp = 10^{-5}c_\parallel$) at 50 to 60°, case (c) ($c_\perp = 10^{-6}c_\parallel$) at around 30°, and case (d) ($c_\perp = 10^{-7}c_\parallel$) at around 10°.

The angle dependence of the spectral index is then compared with that obtained from the single-spacecraft measurements in the solar wind (Horbury et al., 2008; Osman and Horbury, 2009). Overall, case (d) reproduces the observed angle dependence of the spectral index in solar wind turbulence observed by Horbury et al. (2008), in particular the plateau formation at an index of about $-5/3$. Case (b) and (c) also show a partial agreement with the observation by Osman and Horbury (2009) at smaller angles up to $\theta_{VB} = 30°$ and at $\theta_{VB} = 45°$.

The differences in the observed spectral slopes represent different solar wind realizations. The spectra are measured at different radial distances from the Sun, different heliospheric latitudes, and for different components of the fluctuating fields.

Horbury et al. (2008) use a 30-day Ulysses spacecraft data set in the solar wind over Sun's northern polar coronal hole at a heliocentric distance of about 1.4 AU. The plasma is a high-speed solar wind (about 750 km s^{-1}). The spectra are determined for the trace of the cross spectral density matrix in the spacecraft-frame frequency range from about 10^{-2} to about 2×10^{-1} Hz (or in the streamwise wave numbers from about 8×10^{-5} to about 10^{-3} rad km^{-1} using Taylor's frozen-in-flow hypothesis; Taylor, 1938).

Osman and Horbury (2009) use a 1 h Cluster spacecraft data set in 2006 in the near-Earth solar wind (at about 1 AU). The spectra are measured for the perpendicular component to the mean magnetic field. The spacecraft-frame frequency range is above 2×10^{-4} (corresponding to the 1 h interval). The upper limit of the frequency range is not specified in Osman and Horbury (2009). The frequency spectra are averaged over two spacecraft separated at about 10^4 km from each other. The plasma is a low-speed solar wind (about 330 km s^{-1}). The corresponding streamwise wave numbers are above 5×10^{-6} rad km^{-1}.

4 Discussion and conclusion

The concept of the non-elliptic anisotropy is a likely candidate to explain the power-law spectra at arbitrary projection angles from the mean magnetic field and the smooth change in the spectral index from the parallel to the perpendicular projection to the mean magnetic field.

The major lesson from the non-elliptic anisotropy is that the angle dependence of the spectral index can be explained without incorporating the critical balance.

Non-elliptic anisotropy implies that the scale invariance is broken in the wavevector domain such that the sense of anisotropy turns from a parallel extension of the spectrum at lower wave numbers into a perpendicular extension at higher wave numbers.

The broken scale invariance means that the spectrum (or spectral shape) is not self-similar under the simultaneous transformation of the wavevector components $k_\perp \to \lambda k_\perp$ and $k_\parallel \to \lambda k_\parallel$. The non-elliptic anisotropy model breaks the self-similarity in the wavevector domain. The critical balance model (cf. Eq. 3a or 3b in Forman et al., 2011) does not intrinsically retain the self-similar property in the spectral anisotropy for two reasons. First, the dependence on the parallel wavevector components (to the mean magnetic field) is achieved through the positive symmetric function g, while the dependence on the perpendicular wavevector components is made both as a power law and through the function g. Second, the positive symmetric function itself has the scaling invariance because one can renormalize the large-scale parameter L into $L\lambda$ under the transformation $\boldsymbol{k} \to \lambda \boldsymbol{k}$. In the non-elliptic model, the anisotropy becomes stronger at increasingly smaller scales or higher wave numbers due to different power exponents, $k_\perp^2$ and $k_\parallel^3$. The breakdown of the scale invariance may be interpreted as a realization of anisotropic energy cascade or spatially intermittent process that creates sparse structures parallel to the large-scale magnetic field. It is thus important to associate the wavevector spectra with the fluctuation components (waves or coherent structures) and the energy cascade mechanisms.

More detailed verification of the non-elliptic anisotropy is possible using both single-spacecraft and multi-spacecraft methods. In the former case, the angle dependence of the spectral index (as shown in Fig. 3) needs to be evaluated using a larger data set with a higher accuracy in the projection angle resolution and a higher statistical confidence, particularly at small projection angles around 0°. In the latter case, the energy spectra need to be evaluated directly in the wavevector domain. Also, numerical simulation using an MHD code serves as an independent, complementary method to verify the validity of the non-elliptic wavevector anisotropy. As a final remark, we note that further generalizations of the wavevector spectrum should take account of beta dependence, axial asymmetry, and a finite cross helicity.

The topical editor E. Roussos thanks the two anonymous referees for help in evaluating this paper.

References

Abramowitz, M. and Stegun, I. A.: Handbook of Mathematical Functions with Formulas, Graphs, and Mathematical Tables, 9th printing, New York, Dover, 886 pp., 1972.

Bieber, J. W., Matthaeus, W. H., Smith, C. W., Wanner, W., Kallenrode, M.-B., and Wibberenz, G.: Proton and electron mean free paths: The Palmer consensus revisited, Astrophys. J., 420, 294–306, doi:10.1086/173559, 1994.

Bieber, J. W., Wanger, W., and Matthaeus, W. H.: Dominant two-dimensional solar wind turbulence with implications for cosmic ray transport, J. Geophys. Res., 101, 2511–2522, doi:10.1029/95JA02588, 1996.

Biskamp, D.: Magnetohydrodynamic Turbulence, Cambridge University Press, Cambridge, 297 pp., 2003.

Carbone, V., Malara. F., and Veltri, P.: A model for the three-dimensional magnetic field correlation spectra of low-frequency solar wind fluctuations during Alfvénic periods, J. Geophys. Res., 100, 1763–1778, doi:10.1029/94JA02500, 1995.

Chandran, B. D. G.: Strong anisotropic MHD turbulence with cross helicity, Astrophys. J., 685, 646–658, doi:10.1086/589432, 2008.

Chen, C. H. K., Mallet, A., Schekochihin, A. A., Horbury, T. S., Wicks, R. T. and Bale, S. D.: Three-dimensional structure of solar wind turbulence, Astrophys. J., 758, 120, doi:10.1088/0004-637X/758/2/120, 2012.

Dasso, S., Milano, L. J., Matthaeus, W. H., and Smith, C. W.: Anisotropy in fast and slow solar wind fluctuations, Astrophys. J., 635, L181–L184, doi:10.1086/499559, 2005.

Forman, M. A., Wicks, R. T., and Horbury, T. S.: Detailed fit of "critical balance" theory to solar wind turbulence measurements, Astrophys. J., 733, 76, doi:10.1088/0004-637X/733/2/76, 2011.

Goldreich, P., and Sridhar, S.: Toward a theory of interstellar turbulence. 2: Strong alfvenic turbulence, Astrophys. J., 438, 763–775, doi:10.1086/175121, 1995.

Goldreich, P., and Sridhar, S.: Magnetohydrodynamic turbulence revisited, Astrophys. J., 485, 680–688, doi:10.1086/304442, 1997.

Higdon, J. C.: Density fluctuations in the interstellar medium: Evidence for anisotropic magnetohydrodynamic turbulence, I. Model and astrophysical sites, Astrophys. J., 285, 109–123, doi:10.1086/162481, 1984.

Horbury, T. S., Forman, M., and Oughton, S.: Anisotropic scaling of magnetohydrodynamic turbulence, Phys. Rev. Lett., 101, 175005, doi:10.1103/PhysRevLett.101.175005, 2008.

Iroshnikov, P. S.: Turbulence of a conducting fluid in a strong magnetic field, Sov. Astron., 7, 566–571, 1964.

Kolmogorov, A. N.: The local structure of turbulence in incompressible viscous fluid for very large Reynolds number, Dokl. Akad. Nauk. SSSR, 30, 299–303, Reprinted in Proc. Roy. Soc. A, 434, 9–13, doi:10.1098/rspa.1991.0075, 1991, 1941.

Kraichnan, R.: Inertial-range spectrum of hydromagnetic turbulence, Phys. Fluids, 8, 1385–1387, doi:10.1063/1.1761412, 1965.

Matthaeus, W. H., Goldstein, M. L. and Roberts, D. A.: Evidence for the presence of quasi-two-dimensional nearly incompressible fluctuations in the solar wind, J. Geophys. Res., 95, 20673–20683, doi:10.1029/JA095iA12p20673, 1990.

Matthaeus, W. H., and Ghosh, S.: Spectral decomposition of solar wind turbulence: Three-component model, The Solar Wind Nine Conference, AIP Conference Proceedings, edited by: Habbal, S. R., Esser, R., Vollweg, J. V., and Isenberg, P. A., 471, 519–522, doi:10.1063/1.58688, 1999.

Narita, Y., Glassmeier, K.-H., Goldstein, M. L. and Sahraoui, F., Wave-vector dependence of magnetic-turbulence spectra in the solar wind, Phys. Rev. Lett., 104, 171101, 10.1103/PhysRevLett.104.171101, 2010.

Narita, Y., Gary, S. P., Saito, S., Glassmeier, K.-H., and Motschmann, U.: Dispersion relation analysis of solar wind turbulence, Geophys. Res. Lett., 38, L05101, doi:10.1029/2010GL046588, 2011.

Narita, Y., Glassmeier, K.-H., Goldstein, M. L., Motschmann, U., and Sahraoui, F.: Three-dimensional spatial structures of solar wind turbulence from 10 000-km to 100-km scales, Ann. Geophys., 29, 1731–1738, doi:10.5194/angeo-29-1731-2011, 2011.

Narita, Y.: Four-dimensional energy spectrum for space-time structure of plasma turbulence, Nonlin. Processes Geophys., 21, 41–47, doi:10.5194/npg-21-41-2014, 2014.

Narita, Y., Comişel, H., and Motschmann, U.: Spatial structure of ion-scale plasma turbulence, Front. Phys., 2, 13, doi:10.3389/fphy.2014.00013, 2014.

Osman, K. T. and Horbury, T. S.: Multi-spacecraft measurement of anisotropic power levels and scaling in solar wind turbulence, Ann. Geophys., 27, 3019–3025, doi:10.5194/angeo-27-3019-2009, 2009.

Perschke, C., Narita, Y., Gary, S. P., Motschmann, U., and Glassmeier, K.-H.: Dispersion relation analysis of turbulent magnetic field fluctuations in fast solar wind, Ann. Geophys., 31, 1949–1955, doi:10.5194/angeo-31-1949-2013, 2013.

Perschke, C., Narita, Y., Motschmann, U., and Glassmeier, K.-H.: Multi-spacecraft observations of linear modes and sideband waves in ion-scale solar wind turbulence, Astrophys. J. Lett., 793, doi:10.1088/2041-8205/793/2/L25, 2014.

Shebalin, J. V., Matthaeus, W. H., and Montgomery, D.: Anisotropy in MHD turbulence due to a mean magnetic field, J. Plasma Phys., 29, 525–547, doi:10.1017/S0022377800000933, 1983.

Taylor, G. I.: The spectrum of turbulence, Proc. R. Soc. Lond. A, 164, 476–490, doi:10.1098/rspa.1938.0032, 1938.

Wilczek, M. and Narita, Y.: Wave-number-frequency spectrum for turbulence from a random sweeping hypothesis with mean flow, Phys. Rev. E, 86, 066308, doi:10.1103/PhysRevE.86.066308, 2012.

von Papen, M. and Saur, J.: Forward modeling of reduced power spectra from three-dimensional k-space, Astrophys. J., 806, 116, doi:10.1088/0004-637X/806/1/116, 2015.